

# Electron-induced proton knockout from neutron rich nuclei

C. Giusti<sup>1</sup>, A. Meucci<sup>1</sup>, F. D. Pacati<sup>1</sup>, G. Co<sup>2</sup>, V. De Donno<sup>2</sup>,

<sup>1</sup>Dipartimento di Fisica Nucleare e Teorica, Università degli Studi di Pavia and INFN, Sezione di Pavia, via Bassi 6 I-27100 Pavia, Italy

<sup>2</sup>Dipartimento di Fisica, Università del Salento, Lecce, and INFN, Sezione di Lecce, via Arnesano, I-73100 Lecce, Italy

E-mail: [Carlotta.Giusti@pv.infn.it](mailto:Carlotta.Giusti@pv.infn.it)

**Abstract.** We study the evolution of the  $(e, e'p)$  cross section on nuclei with increasing asymmetry between the number of neutrons and protons. The calculations are done within the framework of the nonrelativistic and relativistic distorted-wave impulse approximation. In the nonrelativistic model phenomenological Woods-Saxon and Hartree-Fock wave functions are used for the proton bound-state wave functions, in the relativistic model the wave functions are solutions of Dirac-Hartree equations. The models are first tested against experimental data on  $^{40}\text{Ca}$  and  $^{48}\text{Ca}$  nuclei, and then they are applied to a set of spherical calcium isotopes.

## 1. Introduction

The understanding of the evolution of nuclear properties with respect to the proton to neutron asymmetry is one of the major topics of interest in modern nuclear physics. It is going to extend our knowledge about the effects of isospin asymmetry on the nuclear structure and is also relevant to the study of the origin and the limits of stability of matter in the universe.

Nuclear reactions represent our main source of information on the properties of atomic nuclei. Direct reactions, where the external probe interacts with only one, or a few, nucleons of the target nucleus, give insight into the single-particle (s.p.) properties of the many-body nuclear system. In particular, the  $(e, e'p)$  reaction, where a proton is emitted with a direct knockout mechanism, represents a clean probe to explore the proton-hole states structure of the nucleus [1, 2, 3]. With respect to similar reactions with hadronic probes, such as, e.g., the  $(p, 2p)$  reaction, the  $(e, e'p)$  reaction can exploit the advantages of the electromagnetic interaction, that is well known and relatively weak, if compared with the nuclear interaction.

Several decades of experimental and theoretical work on electron scattering have provided a wealth of information on nuclear structure and dynamics [2, 3]. In the last thirty years many high-resolution exclusive  $(e, e'p)$  experiments [1, 2, 3, 4, 5] have provided accurate information on the s.p. structure of stable closed-shell nuclei. The separation energy and the momentum distribution of the removed proton, which allows to determine the associated quantum numbers, have been obtained. From the comparison between the experimental and theoretical cross sections it has been possible to extract the spectroscopic factors, which give a measurement of the occupation of the different shells and, as a consequence, of the effects of nuclear correlations, which go beyond a mean field (MF) description of nuclear structure.

These studies can be extended to exotic nuclei. In upcoming years the advent of radioactive ion beams facilities will provide a large amount of data on unstable nuclei. A new generation of electron colliders that use storage rings, under construction at RIKEN [6] and GSI [7], will offer unprecedented opportunities to study the structure of exotic unstable nuclei through electron scattering in the ELISE experiment at FAIR [8] and the SCRIT project at RIKEN [9].

In this work models developed and successfully applied to the analysis of the available experimental data for the exclusive  $(e, e'p)$  knockout reactions are used to make predictions for the  $(e, e'p)$  cross sections on exotic nuclei. Our models are based on the distorted-wave impulse approximation (DWIA), within a nonrelativistic and a relativistic framework, and are here applied to a set of calcium isotopes. We have chosen calcium isotopes since data are available from NIKHEF experiments for the doubly magic nuclei  $^{40}\text{Ca}$  and  $^{48}\text{Ca}$  [10, 11]. We first compare our models with these data, then we apply them to some even-even isotopes, *i.e.*,  $^{40,48,52,60}\text{Ca}$  nuclei, where the s.p. levels below the Fermi surface are fully occupied. In this manner we can work with spherical systems and minimize pairing effects. Some results are presented and discussed in the next section. More results can be found in [12]

## 2. Results

Our DWIA calculations have been carried out with the same program DWEEPY [13, 14] which was used for the analyses of the NIKHEF data. The program includes the effects of the final-state interactions (FSI) between the emitted proton and the remaining nucleus, that is described in the calculations by the phenomenological optical potential of [15], as well as the Coulomb distortion of the electron wave functions. Although based on a nonrelativistic DWIA model, DWEEPY contains relativistic effects in the kinematics and in the nuclear current operator. In the comparison with the  $^{40}\text{Ca}(e, e'p)$  and  $^{48}\text{Ca}(e, e'p)$  data we have repeated the original analyses of [10, 11], where the bound-state wave functions are calculated with a phenomenological Woods-Saxon (WS) well whose radius was determined to fit the experimental momentum distribution and whose depth was adjusted to give the experimentally observed separation energy of the bound final state. This choice was able to describe, with a high degree of accuracy, the shape of the experimental momentum distributions at missing-energy values corresponding to specific peaks in the energy spectrum. In order to reproduce the size of the experimental cross sections, reduction factors must be applied to the calculated cross sections. These factors are identified with the spectroscopic factors and their deviation from the predictions of the MF approximation is interpreted as the effect of nucleon-nucleon correlations.

The results obtained with WS wave functions are here compared with those obtained by solving Hartree-Fock (HF) equations with the Gogny-like finite-range D1M interaction [16].

In a third approach we have performed  $(e, e'p)$  calculations with the relativistic DWIA (RDWIA) model of [17, 18, 19, 20, 21, 22], where the s.p. bound-state wave function is the Dirac-Hartree solution from a relativistic Lagrangian written in the context of the relativistic MF theory (RMF) [23] and the scattering wave function is solution of the Dirac equation with the relativistic energy-dependent and A-dependent EDAD1 optical potential [24].

In Fig. 1 our DWIA and RDWIA results are compared with the  $^{40}\text{Ca}(e, e'p)$  and  $^{48}\text{Ca}(e, e'p)$  NIKHEF data [10] for the knockout of a proton from the  $1d_{3/2}$  s.p. level. Data for the  $^{40}\text{Ca}(e, e'p)$  reaction were taken in the so-called parallel and  $(\mathbf{q}, \omega)$  constant kinematics. For the  $^{48}\text{Ca}(e, e'p)$  reaction data were taken only in parallel kinematics. In parallel kinematics the momentum of the outgoing proton  $\mathbf{p}'$  is kept fixed and is taken parallel to the momentum transfer  $\mathbf{q}$ . Different values of the missing momentum  $p_m$ , which is the recoil momentum of the residual nucleus, are obtained by varying the electron scattering angle and, as a consequence,  $q$ . In  $(\mathbf{q}, \omega)$  constant kinematics  $\mathbf{q}$  and the outgoing proton energy are kept constant and different values of  $p_m$  are obtained by varying the angle of the outgoing proton. Experimental data are usually presented as a function of  $p_m$  in terms of the reduced cross section [3], *i.e.*, the cross section divided by a

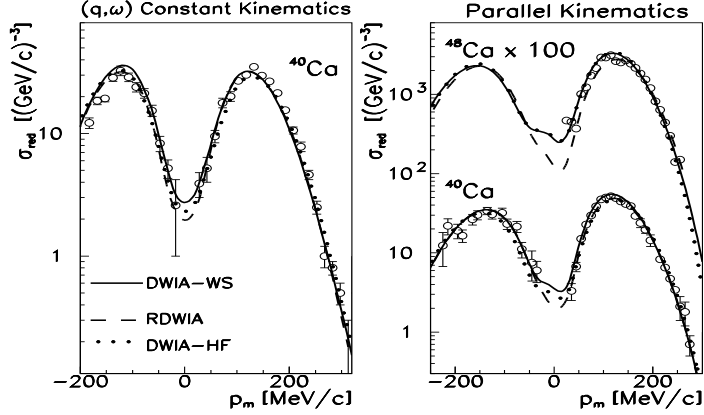


**Figure 1.** Reduced cross sections of the  $^{40}\text{Ca}(e, e'p)$  and  $^{48}\text{Ca}(e, e'p)$  reactions as a function of  $p_m$  for the transition to the  $3/2^+$  ground state of  $^{39}\text{K}$  and to the  $3/2^+$  excited state at 0.36 MeV of  $^{47}\text{K}$  in  $(\mathbf{q}, \omega)$  constant kinematics (left panel), with incident electron energy  $E_0 = 483.2$  MeV, electron scattering angle  $\vartheta = 61.52^\circ$ , and  $q = 450$  MeV/ $c$ , and in parallel kinematics (right panel), with  $E_0 = 483.2$  MeV. The outgoing proton energy is  $T' = 100$  MeV in both kinematics. Line convention: DWIA-WS (solid lines), DWIA-HF (dotted lines), RDWIA (dashed line). The experimental data are taken from [10].

kinematical factor and by the elementary off-shell electron-proton scattering cross section of [25]. In the plane-wave impulse approximation (PWIA), where FSI are neglected and the cross section is factorized into the product of a kinematical factor, the elementary electron-proton scattering cross section, and the hole spectral function, the reduced cross section is the squared Fourier transform of the hole wave function, and can be interpreted as the momentum distribution of the emitted proton when it was inside the nucleus. In DWIA this factorization is destroyed by FSI, but the reduced cross section remains an interesting quantity that can be regarded as the nucleon momentum distribution modified by FSI.

All the theoretical results provide a good description of the shape of the experimental data. A reduction factor has been applied to reproduce the size. This factor has been determined by a fit of the calculated reduced cross sections to the data over the whole missing-momentum range considered in the experiment. The reduction factors applied to the DWIA-WS results (0.49 in  $(\mathbf{q}, \omega)$  constant kinematics and 0.65 in parallel kinematics for  $^{40}\text{Ca}$ , 0.55 for  $^{48}\text{Ca}$ ) are the same as in the data analysis of [10]. The corresponding factors for the DWIA-HF results are 0.51, 0.64, 0.55, and for the RDWIA results are 0.49, 0.69, 0.52. In all the calculations the reduction factors obtained for  $^{40}\text{Ca}(e, e'p)$  reaction in  $(\mathbf{q}, \omega)$  constant kinematics are about 20-25% lower than those obtained in parallel kinematics. The source of this difference is not clear, but it reflects the uncertainties in the identification of the spectroscopic factor as a simple reduction factor of the theoretical results with respect to the experimental data. The reduction factors obtained in all our model calculations for the  $^{48}\text{Ca}(e, e'p)$  reaction are consistently lower than those obtained for the  $^{40}\text{Ca}(e, e'p)$  reaction in the same parallel kinematics.

The predictions of our models for  $1d_{3/2}$  knockout from  $^{40,48,52,60}\text{Ca}$  nuclei in  $(\mathbf{q}, \omega)$  constant and parallel kinematics are shown in Fig. 2. We remark that the evolution of the cross section with respect to the change of the neutron number is the same in all the panels: the  $^{40}\text{Ca}$  lines are always above the other ones, and the size of the curves decreases with the increasing number of neutrons. This behavior is clearer in the DWIA-WS results and becomes less evident in the other cases, especially in the RDWIA ones. The behavior of the s.p. hole wave functions with

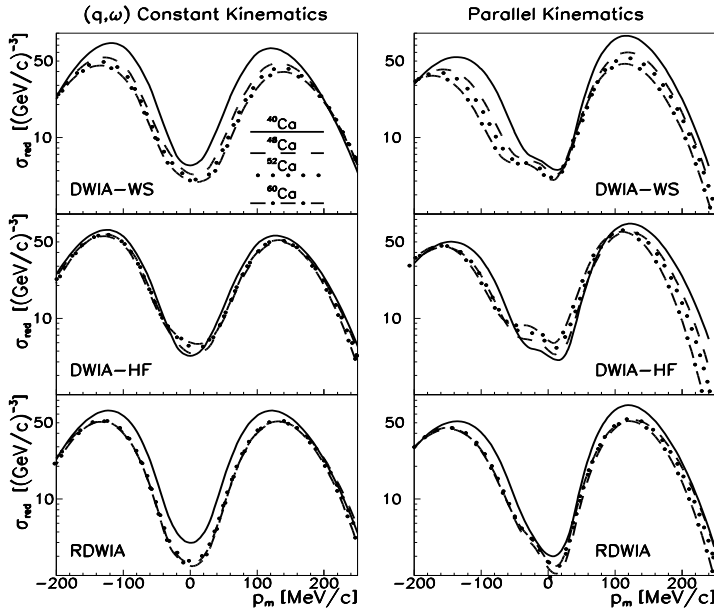


**Figure 2.** Reduced cross section of the  $(e, e'p)$  reaction for  $1d_{3/2}$  knockout from  $^{40}\text{Ca}$  (solid lines),  $^{48}\text{Ca}$  (dashed lines),  $^{52}\text{Ca}$  (dotted lines), and  $^{60}\text{Ca}$  (dot-dashed lines), as a function of  $p_m$ , calculated in  $(\mathbf{q}, \omega)$  constant (left panels) and parallel kinematics (right panels) with DWIA-WS (top panels), DWIA-HF (middle panels), and RDWIA (bottom panels).

increasing neutron number shows a different trend for the different models [12]. The dependence of the wave functions on the proton to neutron asymmetry is responsible for only a part of the differences in the reduced cross sections. While in PWIA the reduced cross section contains only information on the bound-state wave function, in DWIA this information is modified by the contribution of the other ingredients of the model, such as FSI and the electron-nucleon interaction. All these contributions are intertwined in the calculated cross section and, in general, they cannot be easily disentangled. The difference between the results of the two kinematics in Fig. 2 is basically due to the different effects of the distortion produced by the optical potential. These effects strongly depend on kinematics and are larger in parallel than in  $(\mathbf{q}, \omega)$  constant kinematics. Moreover, the trend of the calculated cross sections with the increasing neutron number is significantly affected by the A-dependence of the optical potential [12].

No reduction factor has been applied to the results shown in Fig. 2. The comparison with data in Fig. 1 gives a significant quenching of the measured cross sections with respect to the predictions of the MF model. The quenching is different for the  $^{40}\text{Ca}(e, e'p)$  and  $^{48}\text{Ca}(e, e'p)$  reactions and increases with the neutron number. A quenching depending on the neutron number can be expected for all the isotopes and would give further differences on the reduced cross sections than those shown in Fig. 2.

### 3. Summary and conclusions

We have presented and discussed  $(e, e'p)$  cross sections for a set of calcium isotopes with the aim of studying their evolution with respect to the change of the neutron number.

The nonrelativistic DWIA and relativistic RDWIA models used for the calculations were widely and successfully applied to the analysis of the available  $(e, e'p)$  data over a wide range

of stable nuclei. The results obtained with three different MF descriptions of the hole wave function of the knocked out proton have been compared.

All the three models give a good and similar description of the experimental data on  $^{40}\text{Ca}$  and  $^{48}\text{Ca}$ . The general behavior of the cross sections with respect to the increasing number of neutrons is analogous for all the three models: the reduced cross sections are larger and narrower for the lighter isotopes, and evolve by lowering and widening with increasing neutron number. Although the evolution of the s.p. bound-state wave functions is different for the three models, the dependence of the wave functions on the proton to neutron asymmetry is responsible for only a part of the differences in the calculated cross sections. An important and crucial contribution is also given by FSI, which are described in our models by phenomenological optical potentials. The optical potential affects both the size and the shape of the cross section in a way that strongly depends on kinematics. In particular, its imaginary part, that gives a reduction of the calculated cross section, can affect the values of the spectroscopic factors obtained from the comparison between data and theoretical results. The dependence of the optical potential on the proton to neutron asymmetry is an interesting problem that deserves careful investigation.

From recent studies there are indications that the spectroscopic factors and the effects of correlations depend on the proton to neutron asymmetry. In general, the quenching of quasiparticle orbits, and hence correlations, become stronger with increasing separation energy.

Measurements of the exclusive quasifree ( $e, e'p$ ) cross section on nuclei with neutron excess would offer a unique opportunity for studying the dependence of the properties of bound protons on the neutron to proton asymmetry. The present results can serve as a useful reference for future experiments. The comparison with data can confirm or invalidate the predictions of the model and will test the ability of the established nuclear theory in the domain of exotic nuclei.

This work was partially supported by the MIUR through the PRIN 2009 research project.

## References

- [1] Frullani S, Mougey J 1984 *Adv. Nucl. Phys.* **14** 1
- [2] Boffi S, Giusti C and Pacati F D 1993 *Phys. Rep.* **226** 1
- [3] Boffi S, Giusti C, Pacati F D and Radici M 1996 *Electromagnetic Response of Atomic Nuclei* Oxford Studies in Nuclear Physics, Vol. 20
- [4] Bernheim M *et al.* 1982 *Nucl. Phys. A* **375** 381
- [5] de Witt Huberts P K A *et al.* 1990 *J. Phys. G* **16** 507
- [6] Suda T, Maruyama K, Tanhahata I 2001 *RIKEN Accel. Prog. Rep.* **34** 49
- [7] GSI report 2006, <http://www.gsi.de/GSI-Future/cdr/>
- [8] Antonov A N *et al.* 2011 *Nucl. Instr. and Methods in Physical Research A* **637** 70
- [9] Suda T 2010 *Proposal for Nuclear Physics Experiment at RIBF NP1006-SCRIT01*
- [10] Kramer G J 1990 *Ph.D. thesis, Universiteit Amsterdam*
- [11] Kramer G J, Blok H P, Lapikás L 2001 *Nucl. Phys. A* **679** 267
- [12] Giusti C, Meucci A, Pacati F D, Co' G, De Donno V 2011 *Phys. Rev. C* **84** 014604
- [13] Giusti C, Pacati F D 1987 *Nucl. Phys. A* **473** 717
- [14] Giusti C, Pacati F D 1988 *Nucl. Phys. A* **485** 461
- [15] Schwandt P *et al.* 1982 *Phys. Rev. C* **26** 55
- [16] Goriely S, Hilaire S, Girod M, Péru S 2009 *Phys. Rev. Lett.* **102** 242501
- [17] Meucci A, Giusti C, Pacati F D 2001 *Phys. Rev. C* **64** 014604
- [18] Meucci A, Giusti C, Pacati F D 2001 *Phys. Rev. C* **64** 064615
- [19] Meucci A 2002 *Phys. Rev. C* **65** 464601
- [20] Meucci A, Giusti C, Pacati F D 2002 *Phys. Rev. C* **66** 034610
- [21] Radici M, Meucci A, Dickhoff W H 2003 *Eur. Phys. Jou. A* **17** 65
- [22] Tamae T *et al.* 2009 *Phys. Rev. C* **80** 064601
- [23] Horowitz C J, Murdoch D P, Serot B D 1991 *Computational Nuclear Physics I: Nuclear Structure* Springer-Verlag, Berlin
- [24] Cooper E D *et al.* 1993 *Phys. Rev. C* **47** 297
- [25] de Forest Jr. T 1983 *Nucl. Phys. A* **392** 232